

Anisotropic potential immersed in a dipolar Bose-Einstein condensate

Neelam Shukla¹, Artem G. Volosniev^{2,3}, Jeremy R. Armstrong¹

¹*Department of Physics, University of Nebraska at Kearney, NE-68849 USA*

²*Institute of Science and Technology Austria (ISTA), A-KN-3400, Austria*

³*Department of Physics and Astronomy, Aarhus University,
Ny Munkegade 120, DK-8000 Aarhus C, Denmark*

We study a modified three-dimensional Gross-Pitaevski equation that describes a static impurity in a dipolar Bose-Einstein condensate (BEC). Our focus is on the interplay between the shape of the impurity and the anisotropy of the medium manifested in the energy and the density of the system. Without external confinement, properties of the system are derived with basic analytical approaches. For a system in a harmonic trap, the model is investigated numerically, using the split-step Crank-Nicolson method. Our results demonstrate that the impurity would prefer to change its shape to accommodate the anisotropic character of the bath, in particular it would prefer to align itself with the direction of the dipoles. Our work complements studies of impurities in Bose gases with zero-range interactions, and paves the way for studies of dipolar polarons with a modified Gross-Pitaevski equation.

I. INTRODUCTION

The question of how a system responds to perturbation (stress) is of general importance in physics, in particular, in cold-atom physics. Naturally, isotropic media are the most explored in this context. However, progress in realizing ultracold dipolar gases brings the perfect playground for going beyond isotropicity [1]. It becomes possible to investigate the effect of perturbations on quantum degenerate gases that are intrinsically anisotropic.

In this work, we explore the effect of a static perturbation on an anisotropic medium by placing an impurity at the center of the dipolar Bose gas. The impurity can be an optically generated potential [2–4], which perturbs the host system. By calculating the ensuing properties, we gain insight into the differences between dipolar and non-dipolar systems.

Firstly, we study the Bose gas without external confinement. In this case, the character of the system can be analyzed analytically at least within the local density approximation. We show that even an isotropic impurity leads to an anisotropic response, which reveals the nature of the Bose gas. Further, for an anisotropic impurity, the energy of the system depends strongly on the interplay between the direction of the dipoles and the shape and orientation of the impurity. The dipolar nature of the Bose gas is the most pronounced in the vicinity of the collapse, where the number of bosons displaced by the impurity becomes large. Secondly, we analyze an experimentally relevant system in a harmonic trap. We show that the results derived in the homogeneous setting still hold, advocating for an exploration of static impurities with dipolar gases in a laboratory.

The present manuscript is structured as follows: Section II describes the system and the modified Gross-Pitaevski equation (GPE) used in the study. Section III presents analytical analysis of a Bose gas without external confinement. Section IV contains numerical simulations of the GPE, along with their discussion. Finally, a brief summary of the results and an outlook is given in

Section V. In particular, we propose (and give an example of) a study of the time dynamics that follow a sudden immersion of the impurity. This allows one to estimate timescales relevant for the experiment.

II. FORMALISM

Hamiltonian. The Hamiltonian that describes the system of interest – a Bose gas with a static ‘impurity’ potential – reads

$$H = \sum_{k=1}^N \left[-\frac{\hbar^2}{2m} \frac{\partial^2}{\partial \mathbf{r}_k^2} + V_{\text{trap}}(\mathbf{r}_k) \right] + \sum_{i < j}^N V_c(\mathbf{r}_i - \mathbf{r}_j) + \sum_{i < j}^N V_d(\mathbf{r}_i - \mathbf{r}_j) + \sum_{i=1}^N V_i(\mathbf{r}_i), \quad (1)$$

where m is the mass of a boson, and \mathbf{r}_i is the coordinate of the i th boson. The bosons are confined by the harmonic-oscillator trapping potential V_{trap} . They interact via the contact, V_c , and the dipole-dipole interactions, V_d , discussed below; the function V_i is the impurity-boson potential energy. To differentiate between V_{trap} and V_i , we note that the latter vanishes at infinity, i.e., $V_i(|\mathbf{r}| \rightarrow \infty) \rightarrow 0$.

To analyze the system, we shall rely on a mean-field approximation. Therefore, we can write the contact interaction as $V_c(\mathbf{r}) = 4\pi\hbar^2 a \delta(\mathbf{r})/m$, where a is the scattering length [5, 6]. The functional form of the dipole-dipole potential is

$$V_d(\mathbf{r}) = \frac{\mu_0}{4\pi} \frac{\mathbf{d}^2 - 3(\mathbf{d} \cdot \hat{\mathbf{r}})(\mathbf{d} \cdot \hat{\mathbf{r}})}{|\mathbf{r}|^3}, \quad (2)$$

here \mathbf{d} is the dipole moment of the bosons, μ_0 is the vacuum permeability, and $\hat{\mathbf{r}}$ is the unit vector along the direction of \mathbf{r} . We shall use a system of coordinates in

which the z -axis is along \mathbf{d} , and write the dipole-dipole interaction in a more convenient form

$$V_d = \frac{C_{dd}}{4\pi} \frac{1 - 3\cos^2\theta_d}{r^3}, \quad (3)$$

where θ_d is the angle between \mathbf{r} and \mathbf{d} . We have adopted the standard notation, $C_{dd} = \mu_0 d^2$, which helps us to introduce a relevant length scale (the ‘dipolar length’) as $a_{dd} = C_{dd}m/(12\pi\hbar^2)$ [7]. The Hamiltonian in Eq. (1) without V_i is well-studied [7, 8] theoretically. The focus of our paper is on the effect of the impurity.

Gross-Pitaevski equation. To analyze the system, we rely on a mean-field ansatz, i.e., we assume that the ground state of the Hamiltonian can be approximated by a product state $\psi(\mathbf{r}_1)\psi(\mathbf{r}_2)\dots\psi(\mathbf{r}_N)$ well. To find the function ψ , we solve the GPE

$$-\frac{\hbar^2}{2m} \frac{\partial^2 \psi(\mathbf{r})}{\partial \mathbf{r}^2} + V_{\text{trap}}(\mathbf{r})\psi(\mathbf{r}) + gN|\psi(\mathbf{r})|^2\psi(\mathbf{r}) + N \int d\mathbf{x} V_d(\mathbf{r} - \mathbf{x})|\psi(\mathbf{x})|^2\psi(\mathbf{r}) = (\mu - V_i(\mathbf{r}))\psi(\mathbf{r}), \quad (4)$$

where $g = 4\pi\hbar^2 a/m$ reflects the strength of the contact interaction and μ is the chemical potential. Any solution to the GPE is subject to the normalization condition $\int d\mathbf{r} |\psi(\mathbf{r})|^2 = 1$.

In the next section, we present various approximations for analytical analysis of Eq. (4) in a homogeneous case. In Sec. IV, we calculate the energies and densities in a trapped case. To this end, we solve the GPE using the split-step Crank-Nicolson method. Our numerical code is a modification of an open-source software described in Ref. [9].

III. HOMOGENEOUS SYSTEM

The Thomas-Fermi limit. We start by considering an infinite medium with $V_{\text{trap}} = 0$. We assume that the potential V_i changes ‘weakly and slowly’ (see the discussion below for a weak impurity potential) so that we can employ the Thomas-Fermi approximation and solve the equation

$$V_i(\mathbf{r}) + g\delta n(\mathbf{r}) = - \int d\mathbf{x} V_d(\mathbf{r} - \mathbf{x})\delta n(\mathbf{x}), \quad (5)$$

where $\delta n(\mathbf{x}) = N|\psi(\mathbf{x})|^2 - n_0$ is the change of the density of the Bose gas due to the presence of the impurity, $n_0 = N/\mathcal{V}$ is the density of the gas without the impurity (\mathcal{V} is the volume of the system). Note that we have fixed the chemical potential to its value without the impurity, i.e., $\mu = gn_0$ (it is independent of dipole-dipole interactions in a homogeneous setting). In other words, the density of the Bose gas far from the impurity, n_0 , is independent of the strength of V_i . In this section, we shall use $n_0^{-1/3}$ as the unit of length, and μ as the unit of energy for presenting our findings in a dimensionless form.

Equation (5) has a non-local character, i.e., the density at any given position is determined in part by the density of its surrounding neighborhood. This makes it hard, if not impossible, to solve the equation in real space explicitly. At the same time, linearity of Eq. (5) with respect to δn allows us to find its Fourier transform $\delta\tilde{n}(\mathbf{k}) = \int d\mathbf{r} \delta n(\mathbf{r})e^{-i\mathbf{k}\cdot\mathbf{r}}$ easily:

$$\delta\tilde{n}(\mathbf{k}) = -\frac{\tilde{V}_i(\mathbf{k})}{g + \tilde{V}_d(\mathbf{k})}, \quad (6)$$

where \tilde{V}_i and \tilde{V}_d are Fourier transforms of the impurity and dipole-dipole potentials, respectively. In the case of the dipole potential, $\tilde{V}_d(\mathbf{k}) = C_{dd}(\cos^2\alpha - 1/3)$ [7, 10] with α being the angle between \mathbf{d} and \mathbf{k} . This expression can be conveniently re-written using the second Legendre polynomial: $\tilde{V}_d(\mathbf{k}) = 2C_{dd}P_2(\cos(\alpha))/3$.

The density in real space can be written in integral form as:

$$\delta n(\mathbf{r}) = -\frac{1}{g(2\pi)^3} \int d\mathbf{k} \frac{\tilde{V}_i(\mathbf{k})}{1 + 2\varepsilon_{dd}P_2(\cos\alpha)} e^{i\mathbf{k}\cdot\mathbf{r}}, \quad (7)$$

where $\varepsilon_{dd} = a_{dd}/a$ is a dimensionless ratio that determines the relative importance of dipolar physics. In particular, the system is unstable against a collapse if ε_{dd} is larger or equal to one [7]. Notice that the density is anisotropic even if the impurity potential is isotropic.

To illustrate this, let us consider $\varepsilon_{dd} \rightarrow 0$ (weak dipole-dipole interactions). Using the plane-wave expansion $[e^{i\mathbf{k}\cdot\mathbf{r}} = 4\pi \sum_{l,m} i^l j_l(kr) Y_l^m(\hat{\mathbf{k}})(Y_l^m(\hat{\mathbf{r}}))^*]$ with Y_l^m being the spherical harmonics], we derive

$$\delta n(\mathbf{r}) \simeq -\frac{V_i(\mathbf{r})}{g} - \frac{\varepsilon_{dd}P_2(\cos\theta)}{g\pi^2} \int dk k^2 \tilde{V}_i(k) j_2(kr), \quad (8)$$

where j_l is a spherical Bessel function, and θ is the polar angle of \mathbf{r} . The first term here is the Thomas-Fermi profile for a non-dipolar gas [5]. The second part is due to the dipolar character of the medium; we have used the isotropicity of V_i to simplify it.

The uncomplicated form of Eq. (8) will be modified for larger values of ε_{dd} . In particular, the density will include higher order harmonics, $P_{2n}(\cos\theta)$. We clarify this in Fig. 1 by comparing Eqs. (8) and (7) for a strong spherical Gaussian impurity, $V_i(\mathbf{r}) = \mu \exp(-n_0^{2/3}r^2)$, and different values of ε_{dd} . At small values of ε_{dd} , Eqs. (7) and (8) agree with each other, while becoming more different as the dipolar interaction becomes stronger. They retain similar angular dependence at all values of ε_{dd} . In particular, the density increases (in comparison to n_0) in the direction perpendicular to z , i.e., in the xy -plane. Indeed, it is easier to deform the system in this direction because the corresponding phononic excitations are softer [7].

To further highlight the anisotropic character of Eq. (8), let us study the gradient of the density. In the contact case, we have $\nabla n = \mathbf{F}/g$, where the ‘force’ is

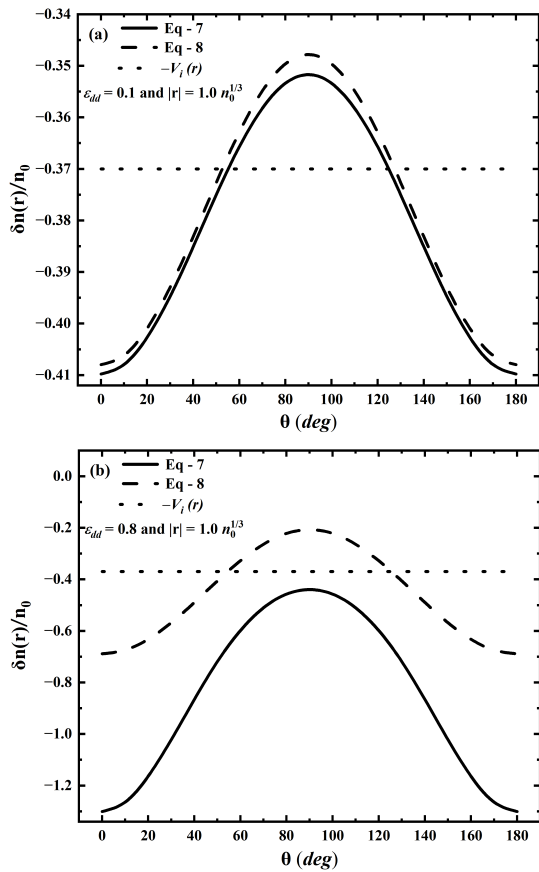


FIG. 1. Comparison of the results obtained from Equations (7) and (8) at different values of ε_{dd} , plotted with respect to the polar angle (θ). The value of the impurity potential is shown with a horizontal dotted line. Note that panel (b) makes it clear that Eq. (8) is not valid for large values of ε_{dd} as $\delta n/n_0 + 1$ must be non-negative (recall that $\delta n + n_0 = N|\psi|^2$).

given by $\mathbf{F} = -\nabla V_i$. This simple law follows from conservation of chemical potential throughout the sample and the fact that the medium is isotropic, so that we cannot assign any tensor to it. For the dipolar medium the situation is different, and the gradient is given not only by the external force, but also by properties of the medium (e.g., internal strain), which are anisotropic and non-local.

Self-energy of the impurity. It is worth noting that Eq. (4) with the reduced mass instead of m can describe also a mobile impurity just as in a non-dipolar case [11–16]. Therefore, even though, our work focuses on the effect of static impurities, our results could also be useful for mobile impurities. Below, we use the densities in the Thomas-Fermi limit to calculate two paradigmatic properties typically studied for mobile impurities. First, we compute the self-energy of the impurity defined as the difference of the energies of the system with and without the impurity:

$$E_{\text{self}} = E[V_i] - E[V_i = 0], \quad (9)$$

where $E[V_i]$ is the energy of the system with the impurity potential V_i . This energy is one of the key characteristics for systems with impurities. Within our approach, E_{self} has the form:

$$E_{\text{self}} = -\frac{gN^2}{2} \int \psi(\mathbf{x})^4 d\mathbf{x} + \frac{g\mathcal{V}n_0^2}{2} - \frac{N^2}{2} \int \psi(\mathbf{x})^2 V_d(\mathbf{r} - \mathbf{x}) \psi(\mathbf{r})^2 d\mathbf{r} d\mathbf{x}, \quad (10)$$

where \mathcal{V} is the volume of the system. After straightforward calculations, we write this expression as

$$E_{\text{self}} = E_{\text{self}}^0 - \frac{1}{2g} \int \delta n(\mathbf{r}) V_d(\mathbf{x} - \mathbf{r}) V_i(\mathbf{x}) d\mathbf{r} d\mathbf{x}, \quad (11)$$

where $E_{\text{self}}^0 = n_0 \int V_i(\mathbf{r}) d\mathbf{r} - \frac{1}{2g} \int V_i^2(\mathbf{r}) d\mathbf{r}$ is the contribution to the energy that is independent of the dipolar nature of the Bose gas. Let us assume that the dipole-dipole interactions are weak (i.e., $\varepsilon_{dd} \rightarrow 0$), then we can estimate the dipolar contribution to the self-energy as

$$E_{\text{self}} - E_{\text{self}}^0 \simeq \frac{1}{2g^2} \int V_i(\mathbf{r}) V_d(\mathbf{x} - \mathbf{r}) V_i(\mathbf{x}) d\mathbf{r} d\mathbf{x}. \quad (12)$$

This equation clearly shows that the self-energy depends not only on the anisotropy of the dipole-dipole interactions, but also on the anisotropy of the impurity potential. Indeed, if the potential V_i is elongated along the z -direction, then the right-hand-side of Eq. (12) is negative. The opposite is true for the impurity potentials elongated along the x -axis. We shall illustrate this dependence numerically in the next section for a trapped system.

Number of bosons in a ‘dressing’ cloud. The number of bosons directly affected by the presence of the impurity can be estimated as follows ($\delta N = \int d\mathbf{r} \delta n(\mathbf{r})$)

$$\delta N = -\frac{\int d\mathbf{r} V_i(\mathbf{r})}{g\sqrt{3\varepsilon_{dd}(1 - \varepsilon_{dd})}} \tan^{-1} \left[\sqrt{\frac{3\varepsilon_{dd}}{1 - \varepsilon_{dd}}} \right]. \quad (13)$$

This expression shows that $|\delta N|$ is an increasing function of ε_{dd} , implying that the dipolar medium leads to a ‘more heavy’ dress of the impurity. This can be most easily visualized by considering limiting cases. For weak dipole-dipole interactions, $\varepsilon_{dd} \rightarrow 0$, we derive

$$\delta N \simeq -\frac{1}{g} \int d\mathbf{r} V_i(\mathbf{r}) \left(1 + \frac{4\varepsilon_{dd}^2}{5} \right). \quad (14)$$

Note that this expression depends on the square of ε_{dd} , because the linear contribution from Eq. (8) averages out to zero. In the vicinity of the collapse, $\varepsilon_{dd} \rightarrow 1$,

$$\delta N \simeq -\frac{\pi \int d\mathbf{r} V_i(\mathbf{r})}{2\sqrt{3}g\sqrt{1 - \varepsilon_{dd}}}. \quad (15)$$

This result is likely beyond the limits of applicability of local-density approximation, see below. Still, it shows

that the number of bosons in the dressing cloud becomes large close to collapse. For a mobile impurity, this should lead to strong renormalization of the effective mass in agreement with previous studies of dipolar Bose polarons [17–19]. The mass renormalization is however direction-dependent with the strongest effect in the xy -plane, which cannot be captured by the angle-averaged quantity δN .

Weak impurity potentials. Finally, we briefly discuss the limits of applicability of the Thomas-Fermi approximation. To this end, we study a weak impurity potential, namely, we consider Eq. (4) without a trap and $V_i \rightarrow 0$. We look for the solution ψ in the following form (cf. Ref. [20]):

$$\psi(\mathbf{r}) \simeq \frac{1 + f(\mathbf{r})}{\sqrt{\mathcal{V}}}. \quad (16)$$

We assume that f is small, and satisfies the equation

$$\frac{\hbar^2}{2m} \nabla^2 f(\mathbf{r}) = 2\mu f + \frac{2\mu}{g} \int d\mathbf{x} V_d(\mathbf{r} - \mathbf{x}) f(\mathbf{x}) + V_i, \quad (17)$$

which allows us to find Fourier transform $\tilde{f}(\mathbf{k})$ as

$$\tilde{f}(\mathbf{k}) = -\frac{\tilde{V}_i(\mathbf{k})}{\frac{\hbar^2 k^2}{2m} + 2\mu + \frac{2\mu}{g} \tilde{V}_d(\mathbf{k})}. \quad (18)$$

By comparing this equation to Eq. (6), we conclude that the Thomas-Fermi approximation is valid if the characteristic momenta of $V_i(\mathbf{k})$ are much smaller than $\sqrt{4\mu m/\hbar^2} \sqrt{1 + 2\varepsilon_{dd} P_2(\cos \alpha)}$. It is clear that this condition depends strongly on ε_{dd} . In particular, for ε_{dd} close to one, $1 + 2\varepsilon_{dd} P_2(0)$ is small and the Thomas-Fermi approximation should be used with great care.

Finally, we mention another indication that the local-density approximation fails, which follows from the observation that $\delta n(\mathbf{r})/n + 1$ should be non-negative. Assuming repulsive spherically symmetric impurity with its maximum at the origin, the fulfillment of this condition can be checked by considering $\delta n(0)/n + 1$, which using Eq. (7) leads to

$$1 - \frac{\int dk \tilde{V}_i(k) k^2}{2\pi^2 \mu \sqrt{3\varepsilon_{dd}(1 - \varepsilon_{dd})}} \tan^{-1} \left[\sqrt{\frac{3\varepsilon_{dd}}{1 - \varepsilon_{dd}}} \right] \geq 0. \quad (19)$$

This condition clearly fails when the impurity is too strong, $V_i(0) \gtrsim \mu$, or when the system is close to the dipolar collapse, $\varepsilon_{dd} \rightarrow 1$.

IV. TRAPPED SYSTEM

Guided by the results above, we now conduct a detailed analysis across a range of scenarios, which should help to identify the physics described in the previous section in a laboratory. To this end, we consider a harmonically trapped system of dysprosium atoms whose large

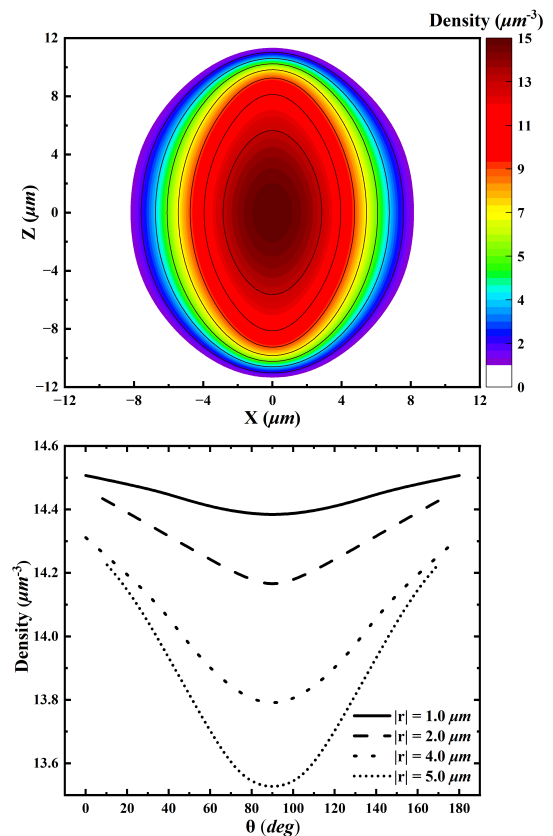


FIG. 2. Density distribution of the BEC in the absence of the impurity potential. Panel (a) shows the density in the xz -plane. Panel (b) shows the density for a given value of $|r|$ as a function of the polar angle.

dipolar length $a_{dd} \approx 130a_0$ puts them at the forefront of current experimental studies [1]. For simplicity, the trapping potential is assumed to be symmetric, with the form given by:

$$V_{\text{trap}} = \frac{1}{2} m \omega^2 r^2, \quad (20)$$

where ω is the trapping frequency. The corresponding harmonic oscillator length is $L = \sqrt{\hbar/(m\omega)}$. In our numerical simulations, we use $L = 1\mu\text{m}$, which is representative of experimentally relevant values [21]. We set the number of atoms to $N = 2 \times 10^4$. The atomic scattering length is chosen to be $a = 150a_0$, which makes the gas stable ($a > a_{dd}$). This a is close to the background value in ^{162}Dy samples, otherwise our choice is rather arbitrary as a can be tuned using external magnetic fields, see, e.g., Ref. [1].

In Fig. 2, the density distribution of the dipolar gas in the absence of the impurity is shown in the xz -plane, parallel to the plane of polarization. As expected [22, 23], the graph demonstrates that the intrinsic interactions between the dipoles of the system make the system elongated along the z -axis, the direction in which the dipoles are polarized. We stress that the trap itself is isotropic, so

that the anisotropy observed in the density is purely from the interactions within the system (cf. Sec. III). For the considered parameters of the Bose gas, this anisotropy is weak close to the origin (see, e.g., the almost flat curve at $|\mathbf{r}| = 1\mu\text{m}$ in Fig. 2b)), providing a suitable testbed for investigating the anisotropy induced by the impurity.

A. Introducing the Impurity

We assume an impurity described by the potential

$$V_i(x, y, z) = V_0 \exp \left[- \left(\frac{x^2 + y^2}{a^2 L^2} + \frac{z^2}{b^2 L^2} \right) \right]. \quad (21)$$

Here, a and b parameterize the width of the impurity potential in the transverse and longitudinal directions. The parameter V_0 determines the strength of the impurity potential. It was set to be $5\hbar\omega$ in our calculations, implying that the effect of the impurity is strong (non-perturbative), i.e., a number of collective modes can be excited in the Bose gas. The potential in Eq. (21) can be produced in a cold Bose gas by a laser beam [2–4], providing a physical realization of the impurity studied here in a laboratory.

First, to understand the effect of the static impurity on the BEC, we calculate the density of the Bose gas for various deformation ratios. Here, the “deformation ratios” refer to a systematic variation in the values of a and b in Eq. (21), while keeping the volume of the impurity ($4\pi a^2 b L^3/3$, treating it as an ellipsoid) constant at $1\mu\text{m}^3$. The volume integral of the potential, $\int d\mathbf{r} V_i(\mathbf{r})$, is then also constant at $3V_0 L^3 \sqrt{\pi}/4$. We showed in Sec. III that the volume integral of the impurity is a crucial property of the potential that determines the energy of the system in the homogeneous case. Therefore, by fixing it we can more directly see the effect of the dipolar nature of the bath, i.e., we can isolate the effect of the last term in Eq. (11). [Note however that the interplay between the external trap and the impurity potential also plays an important role in the results presented in this section.] For the sake of simplicity, here we will mostly discuss results for $a = b$, $a = 3b/2$, and $a = 3b$.

Figure 3(a) illustrates the scenario of an isotropic impurity ($a = b$), as evidenced by the circular contours at the origin. The emergence of two central peaks shows the effect of the static impurity repelling the dipoles away from the origin. The peaks of the densities are located along the $z=0$ lines in agreement with the discussion in Sec. III (see in particular Fig. 1). Further away from the impurity, the density is dominated by the harmonic trap (cf. Fig. 2).

Figures 3(b)-(c) display results for anisotropic impurity potentials ($a \neq b$), with the impurity elongated along the x -axis, which induces a competition between intrinsic anisotropy of the system and anisotropy of the impurity. The elongation of the impurity dominates the properties of the dipolar gas at the origin. In particular, we see that

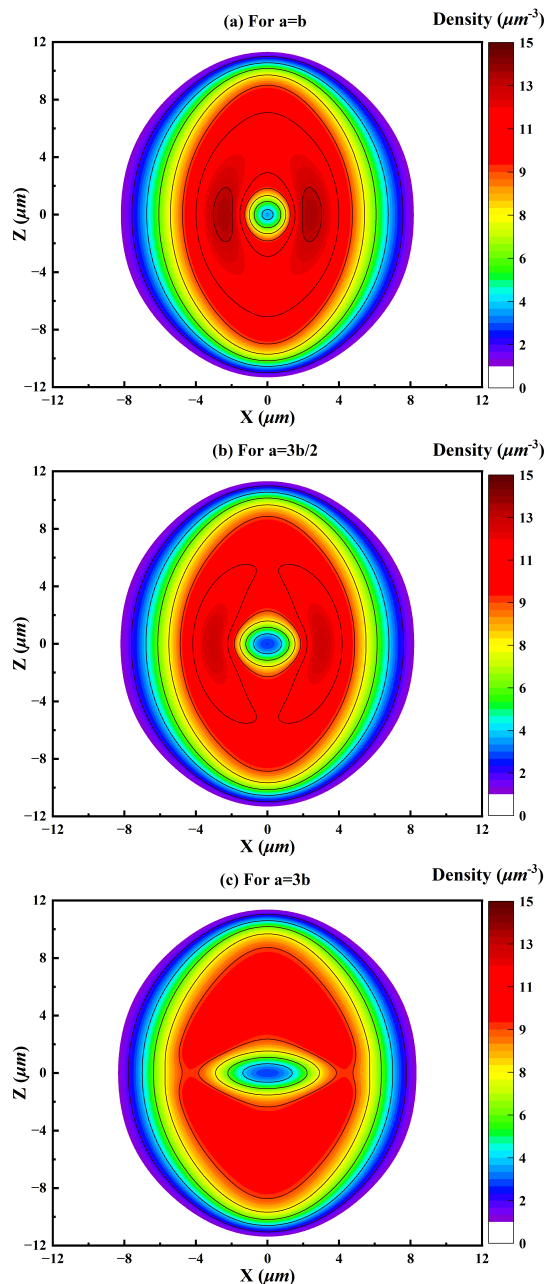


FIG. 3. Density of the system (BEC + static impurity) in the xz -plane for different deformation ratios a/b , cf. Eq. (21).

contour plots of the density are elongated predominantly along the x -axis in the vicinity of the origin.

In Fig. 3(c), which represents the maximum deformation analyzed in this study, the peaks in density are now distinctly separated along the $\pm z$ -axis, though they appear smaller and much broader than the other cases. The large deformation of the impurity has forced the system to reconstitute itself away from the x -axis and assemble in broad peaks separated along the dipolar axis. While the behavior far from the impurity remains similar to the previous cases, the system’s response in the region

of the impurity is clearly dependent on the precise shape and orientation of the impurity, the latter property we explore in the next section.

B. Orientation-Dependent Effects of Impurity

To further analyze the interplay between the anisotropy of the impurity and the dipolar nature of the bath, in particular, the restoring of the dipolar symmetry far from the impurity, we examine the effect of rotating the impurity about the y -axis. To achieve this, we employ a rotation matrix to change the functional form of the impurity potential in Eq. (21). As a result, we obtain:

$$V_i = V_0 \exp \left[- \left(\frac{(x \cos \varphi + z \sin \varphi)^2 + y^2}{a^2 L^2} + \frac{(z \cos \varphi - x \sin \varphi)^2}{b^2 L^2} \right) \right], \quad (22)$$

where, the angle φ is defined relative to the x -axis. Note that neither the volume of the impurity ($4\pi a^2 b L^3/3 = 1\mu\text{m}^3$) nor the volume integral of the potential change by rotation.

We present densities for 30° , 60° , and 90° fixing $a = 3b/2$ in Fig. 4. All these results exhibit similar features to those discussed in Fig. 3. Furthermore, they demonstrate the rotation of the density driven by the angle φ . For example, as the angle increases, the center appears to rotate and align with that particular angle. The density contours almost appear 'stirred' though the impurity is static. The contours in the case of the top two panels also show the gradual evolution from the shape and orientation of the impurity to that of the bath. In the bottom panel, the impurity's elongation matches the elongation of the trap, so the center contours' orientation matches that of the edge contours. In addition, the peaks become sharper as the major axis gets closer to aligning with the polarization direction.

A superficial visual inspection of the density contours suggests that the maximum effect of the impurity potential occurs when the impurity's major axis is orthogonal to the polarization of the dipoles and decreases as they become more aligned. This remains true even for larger deformations of the impurity (not shown). To quantify this observation, we calculate the energy of the system below.

C. Self-Energy of Impurity

The results above show the interplay between the anisotropy of the impurity and the anisotropy of the medium in a trap. Quantifying this interplay by looking at the densities is difficult. Therefore, in this subsection, we study the energy of the system. To quantify this effect, we calculate the self-energy (E_{self}) defined as in Sec. III. We expect this quantity to depend not only on

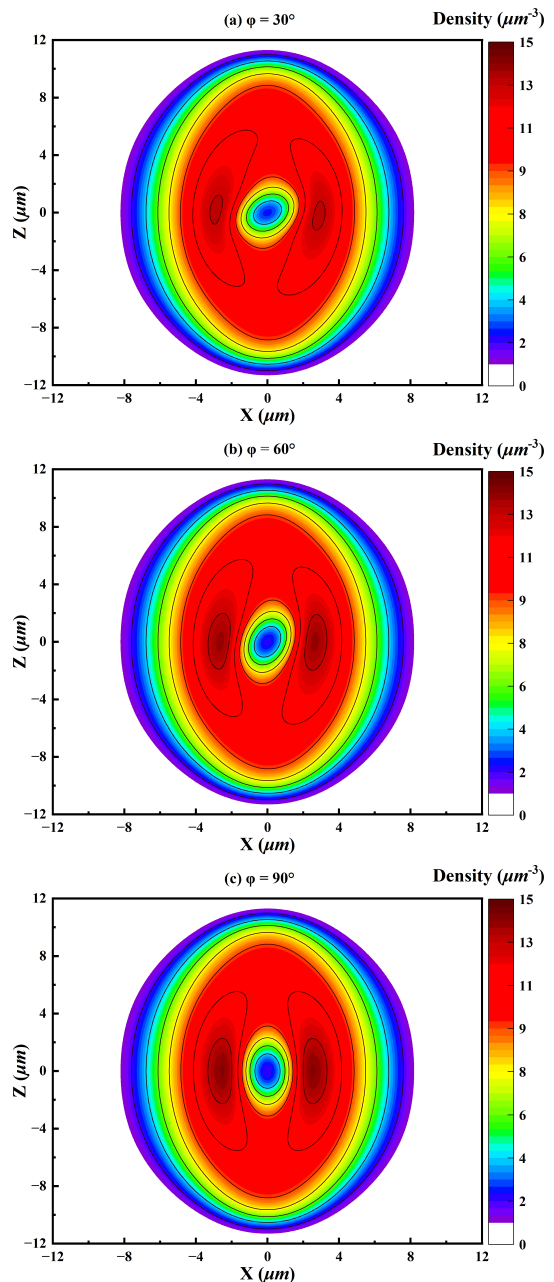


FIG. 4. Density of the system (BEC + static impurity) in the xz -plane for different orientations of the impurity, i.e., for different values of φ , cf. Eq. (22). The deformation ratio is $a = 3b/2$ here.

the amount of deformation but also on the orientation of the impurity.

In Figure 5, the self-energy of the impurity for several deformation ratios is presented with respect to various orientation angles. The self-energy of the impurity-BEC system exhibits a nearly sinusoidal variation, showing a strong preference for the major axis of the impurity deformation to align along the z -axis (cf. Eq. (12)). The effect is solely due to the dipolar nature of the condensate, and

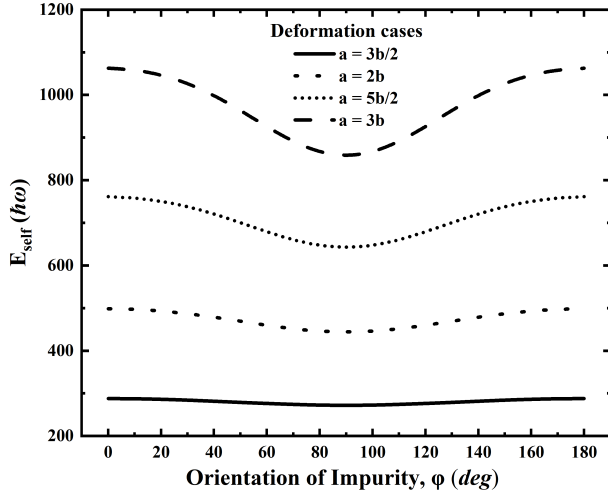


FIG. 5. Effect of rotation on the self-energy of the impurity for different deformation ratios. Recall that the orientation angle is defined with respect to the x -axis and that the volume integral of the impurity ($\int d\mathbf{r}V_i(\mathbf{r}) = 3V_0L^3\sqrt{\pi}/4$) is fixed, cf. Eq. (22).

vanishes if $\varepsilon_{dd} = 0$. Larger deformation ratios exhibit very similar qualitative behavior, though quantitatively all the self-energies increase with increasing deformation.

We illustrate this in Figure 6, which demonstrates the dependence of the self-energy on the major and minor axis ratio, a/b . This plot echoes what was seen in Figure 5, in that the most energetically favorable impurity is the one with the most elongation along the polarization axis. The prolate ($a < b$) impurity allows more of the dipoles to be closer together in their favored head-to-tail configuration. Once the impurity becomes isotropic and then oblate ($a > b$), the self-energy increases more rapidly as the impurity's presence is increasingly disruptive to the dipolar gas. The dashed line in Figure 6 shows the self-energy results for the systems where the impurity has been rotated by 90° . Here we see that for the oblate case, rotating the impurity decreases the self-energy. Since after rotating 90° , the impurity's major axis is now along the z -axis, this result is not surprising. In the case of the prolate impurity, we observe the opposite in that the rotation increases the self-energy. The reasoning is the same since now the longest axis is along the x -axis, though the difference is less dramatic than in the oblate case.

V. CONCLUSION AND OUTLOOK

We have investigated the response of a dipolar medium to an implantation of a repulsive impurity at its center. We have observed a large distortion to the density of the medium, which indicates a preference for the dipoles to stay in their preferred head-to-tail configuration. This

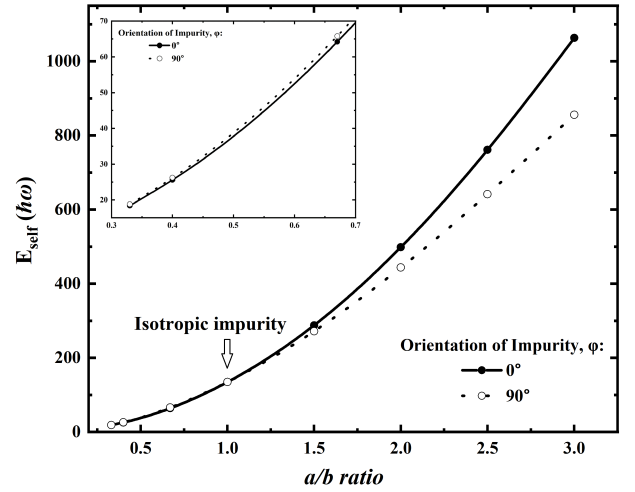


FIG. 6. Self-energies plotted as a function of the deformation ratio, a/b , for two orientations of the impurity potential in Eq. (22). The inset zooms in on small a/b ratios.

preference is reinforced by our results for self-energy, which we have examined as a function of the deformation of the impurity as well as the orientation of the impurity. Our results pave the way for a number of possible follow-up studies some of which we briefly outline below.

Mixtures. Mixtures of dipolar Bose gases with non-dipolar Bose or Fermi gases received relatively little attention in spite of their potentially rich physics [24, 25]. Recent progress in realizing quantum mixtures of dipolar gases [26] may, however, motivate further exploration of such systems.

Inadvertently, our results provide insight into properties of two-component mixtures. Arguably, the simplest mixture is an impurity system – a dipolar polaron [17–19] – that was mentioned already in Sec. III. The self-energy in Eq. (12) suggests that the induced impurity-impurity interaction becomes long-range. Indeed, assuming that the $V_i = v_1 + v_2$, where v_1 and v_2 correspond to two impurities, we derive the dipole-interaction-induced part of the mediated interaction as

$$V_{\text{eff}} \simeq \frac{1}{g^2} \int v_1(\mathbf{r})V_d(\mathbf{x}-\mathbf{r})v_2(\mathbf{x})d\mathbf{r}d\mathbf{x}, \quad (23)$$

which, assuming that $v_j(\mathbf{r}) = g_j\delta(\mathbf{r}-\mathbf{a}_j)$, leads to $V_{\text{eff}} \simeq g_1g_2V_d(\mathbf{a}_1-\mathbf{a}_2)/g^2$. This interaction is of long-range in contrast to the well-known mean-field effective impurity-impurity interactions, see, e.g., [27–31]. In the future it will be interesting to investigate this potential in the vicinity of the collapse where the impurity can strongly modify the bath.

Finally, we note that one can naively think of the impurity potential in Eq. (21) as of some zero-range-interacting Bose or Fermi gas that does not mix with the dipolar BEC, for conditions of miscibility of Bose-Bose mixtures see Ref. [32]. In this case, our study provides

some ideas for understanding immiscible two-component gases, where one of the gases (impurity) has only zero-range interactions. For example, Figure 6 suggests that the density of this impurity gas will be shaped by the dipolar interaction.

Time dynamics. Another interesting question is how the system evolves once an impurity is introduced (going from Figure 2 to Figure 3). To do this, we start with the density solution of our system without an impurity and then utilize the real-time propagation of the split-step Crank-Nicolson method for our numerical solutions. The results of this can be seen in Figure 7, where the density in 1D cross sections along the x - and z -axes are shown. There it can be seen how the density plunges in the center of the trap by first creating large peaks close to the origin, which then recede over longer times as more particles are pushed away from the repulsive impurity and vacate the center region of the trap. The 'static result' would be the eventual profile reached at long times once the transient effects of the placement of the impurity resolve. We should emphasize that these time dynamics results are preliminary and serve as an invitation to further study.

ACKNOWLEDGEMENTS

The authors acknowledge that this material is based upon work supported by the National Science Foundation/EPSCoR RII Track-1: Emergent Quantum Materials and Technologies (EQUATE), Award OIA-2044049.

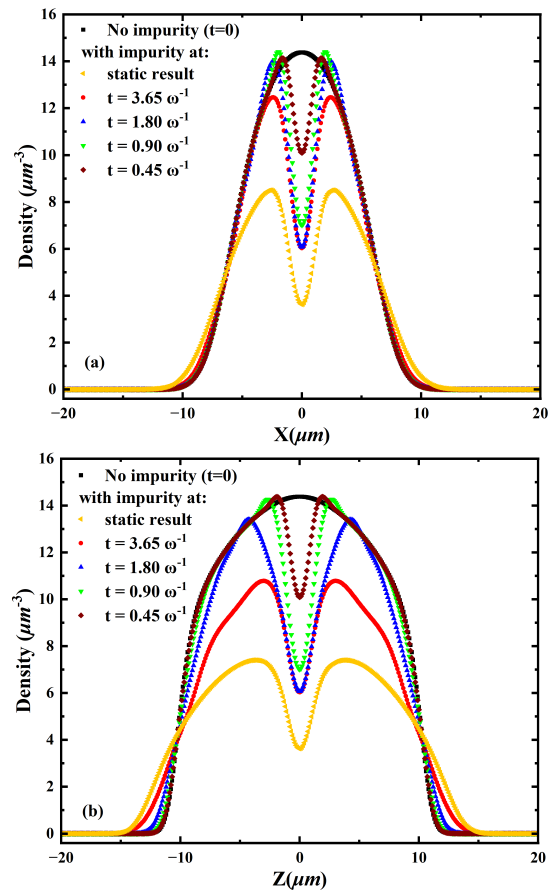


FIG. 7. Density profiles along the x -axis (upper panel) and z -axis (lower panel) for different amounts of time evolution. At $t = 0$, a dipolar BEC without an impurity has a spherical impurity implanted into it at the origin. Note that the important timescale is defined by the frequency of the external trap, ω , which sets the smallest energy scale of the system. For the Dy system, which we use in our numerical simulations, $1/\omega \simeq 2.5$ ms.

-
- [1] L. Chomaz, I. Ferrier-Barbut, F. Ferlaino, B. Laburthe-Tolra, B. L. Lev, and T. Pfau, Reports on Progress in Physics **86**, 026401 (2022).
 - [2] M. R. Andrews, D. M. Kurn, H.-J. Miesner, D. S. Durfee, C. G. Townsend, S. Inouye, and W. Ketterle, Physical Review Letters **79**, 553–556 (1997).
 - [3] D. M. Stamper-Kurn, H.-J. Miesner, A. P. Chikkatur, S. Inouye, J. Stenger, and W. Ketterle, Physical Review Letters **81**, 2194–2197 (1998).
 - [4] S. Stellmer, B. Pasquiou, R. Grimm, and F. Schreck, Physical Review Letters **110**, 263003 (2013).
 - [5] F. Dalfovo, S. Giorgini, L. P. Pitaevskii, and S. Stringari, Rev. Mod. Phys. **71**, 463 (1999).
 - [6] E. Braaten and H.-W. Hammer, Physics Reports **428**, 259–390 (2006).
 - [7] T. Lahaye, C. Menotti, L. Santos, M. Lewenstein, and T. Pfau, Reports on Progress in Physics **72**, 126401 (2009).
 - [8] M. A. Baranov, M. Dalmonte, G. Pupillo, and P. Zoller, Chemical Reviews **112**, 5012–5061 (2012).
 - [9] R. K. Kumar, L. E. Young-S, D. Vudragović, A. Balaž, P. Muruganandam, and S. K. Adhikari, Computer Physics Communications **195**, 117 (2015).
 - [10] K. Góral, K. Rzażewski, and T. Pfau, Phys. Rev. A **61**, 051601 (2000).
 - [11] E. Gross, Annals of Physics **19**, 234 (1962).
 - [12] A. G. Volosniev and H.-W. Hammer, Phys. Rev. A **96**, 031601 (2017).
 - [13] O. Hryhorchak, G. Panochko, and V. Pastukhov, Journal of Physics B: Atomic, Molecular and Optical Physics **53**,

- 205302 (2020).
- [14] J. Jager, R. Barnett, M. Will, and M. Fleischhauer, *Phys. Rev. Res.* **2**, 033142 (2020).
- [15] M. Drescher, M. Salmhofer, and T. Enss, *Phys. Rev. Res.* **2**, 032011 (2020).
- [16] N.-E. Guenther, R. Schmidt, G. M. Bruun, V. Gurarie, and P. Massignan, *Phys. Rev. A* **103**, 013317 (2021).
- [17] B. Kain and H. Y. Ling, *Physical Review A* **89**, 023612 (2014).
- [18] L. A. P. Ardila and T. Pohl, *Journal of Physics B: Atomic, Molecular and Optical Physics* **52**, 015004 (2018).
- [19] A. G. Volosniev, G. Bighin, L. Santos, and L. A. Peña Ardila, *SciPost Physics* **15** (2023).
- [20] B. Nikolić, A. Balaž, and A. Pelster, *Phys. Rev. A* **88**, 013624 (2013).
- [21] M. Lu, N. Q. Burdick, S. H. Youn, and B. L. Lev, *Phys. Rev. Lett.* **107**, 190401 (2011).
- [22] S. Yi and L. You, *Phys. Rev. A* **61**, 041604 (2000).
- [23] L. Santos, G. V. Shlyapnikov, P. Zoller, and M. Lewenstein, *Phys. Rev. Lett.* **85**, 1791 (2000).
- [24] O. Dutta and M. Lewenstein, *Phys. Rev. A* **81**, 063608 (2010).
- [25] B. Kain and H. Y. Ling, *Phys. Rev. A* **83**, 061603 (2011).
- [26] A. Trautmann, P. Ilzhöfer, G. Durastante, C. Politi, M. Sohmen, M. J. Mark, and F. Ferlaino, *Phys. Rev. Lett.* **121**, 213601 (2018).
- [27] M. Bruderer, A. Klein, S. R. Clark, and D. Jaksch, *New Journal of Physics* **10**, 033015 (2008).
- [28] P. Naidon, *Journal of the Physical Society of Japan* **87**, 043002 (2018).
- [29] F. Brauneis, H.-W. Hammer, M. Lemeshko, and A. G. Volosniev, *SciPost Phys.* **11**, 008 (2021).
- [30] A. Petković and Z. Ristivojevic, *Phys. Rev. A* **105**, L021303 (2022).
- [31] M. Will, G. E. Astrakharchik, and M. Fleischhauer, *Phys. Rev. Lett.* **127**, 103401 (2021).
- [32] R. K. Kumar, P. Muruganandam, L. Tomio, and A. Gammal, *Journal of Physics Communications* **1**, 035012 (2017).